

From tunneling to point contact: Correlation between forces and current

Yan Sun, Henrik Mortensen, Sacha Schär, Anne-Sophie Lucier, Yoichi Miyahara, and Peter Grütter
Department of Physics, McGill University, 3600 University Street, Montreal, Quebec, H3A 2T8, Canada

Werner Hofer

Surface Science Research Centre and the Department of Physics, University of Liverpool, United Kingdom

(Received 7 February 2005; published 25 May 2005)

We used a combined ultrahigh vacuum scanning tunneling and atomic force microscope (STM/AFM) to study W tip-Au(111) sample interactions in the regimes from weak coupling to strong interaction and simultaneously measure current changes from picoamperes to microamperes. Close correlation between conductance and interaction forces in a STM configuration was observed. In particular, the electrical and mechanical points of contact are determined based on the observed barrier collapse and adhesive bond formation, respectively. These points of contact, as defined by force and current measurements, coincide within measurement error. *Ab initio* calculations of the current as a function of distance in the tunneling regime is in quantitative agreement with experimental results. The obtained results are discussed in the context of dissipation in noncontact AFM as well as electrical contact formation in molecular electronics.

DOI: 10.1103/PhysRevB.71.193407

PACS number(s): 73.40.Jn, 68.35.Gy, 68.37.Ef, 68.37.Ps

Scanning probe microscopes, such as scanning tunneling microscopes (STM) and atomic force microscopes (AFM) are central tools for atom/molecule manipulation and characterization in nanotechnology.¹ Furthermore, a STM tip can also be considered as a mobile electrode in the burgeoning field of nanoelectronics, where it is widely accepted that the role of contacts is the crucial unknown.^{2,3} It is thus of fundamental and practical importance to understand the interactions between a probing tip and a sample under well-defined conditions.

Tremendous theoretical and experimental efforts have been made to investigate tip-sample interaction at the atomic scale; however, many important aspects are still not well understood.^{4–17} The transition from tunneling to electrical contact is not fully characterized or understood, partially due to variations of the experimental setups and the assumptions made in theoretical models.^{7–11,18} Correlations between the tunneling current and atomic forces have been investigated theoretically and experimentally.^{4–6,11,13,15} The short decay length and associated mechanical jump-to-contact caused by adhesive interaction forces, predicted by many theories, is not always observed.^{14–17} The formation and central role of electrical contacts in molecular electronics is only poorly understood.^{2,3} Finally, the interpretation of energy dissipation at short ranges often experimentally observed in noncontact (NC) AFM is highly controversial.¹⁹

In this work, we investigate the force and current between a W tip and a Au(111)- $22 \times \sqrt{3}$ reconstructed surface by simultaneous STM and AFM measurements as a function of tip-sample separation (z) at room temperature under UHV conditions ($p < 1 \times 10^{-10}$ mbar). We present measurements from large separations up to the formation of an electrical and mechanical contact. For the experiments described below, we used an improved version of the combined UHV STM/AFM setup described in Ref. 20. In particular, an I - V converter capable of measuring currents from 1 pA to 10 mA was implemented.²¹ Previously, the measured cur-

rents were limited to 100 nA, precluding a study of the conductance behavior at or near contact.¹⁵ Prior to measurements, the tip was annealed by passing a dc current through the tip shank to anneal the tip and remove residual oxides from the etching process. The tip was then negatively biased relative to an electron collection disk 2.5 cm away until a stable field emission current of 10 nA was observed. Based on the Fowler-Nordheim plot, the tip radius, cross-checked by field-ion microscopy, was estimated to be 3–15 nm.²² The sample was a 100 nm gold film thermally evaporated on a sheet of mica (5 mm by 2.5 mm by 0.05 mm, grade V1, SPI Supplies) at high vacuum (1×10^{-6} mbar). Both sides of mica were coated using the same conditions (details in Ref. 23) and was used as sample and a force sensor by optically detecting its deflection. Deflections were detected directly using an *in situ* interferometer with a noise floor of less than 0.02 nm rms in a 0–2 kHz bandwidth.^{20,22} The effective spring constant was determined to be 45 ± 15 N/m at the point where the tip approached the sample surface. Upon transfer to the UHV chamber, cycles of sputtering and annealing were applied to the Au sample until no detectable contamination was found by Auger electron spectroscopy.

With our feedback loop,²⁴ the following spectroscopy sequence was implemented. Starting from a reference point defined by a tunneling current of 60 pA at a bias of 50 mV, the feedback was switched off and the tip-sample separation increased by a predetermined amount. While simultaneously recording the current $I(z)$ and the cantilever deflection [proportional to force $F(z)$] the tip was approached towards the surface at a rate of 1 to 2 nm/s for a predetermined distance and subsequently retracted by the same amount. After completion of each approach and retraction cycle, the feedback was switched on again and tunneling stabilized at 60 pA for 0.5 s. After a few cycles of approach and retraction, the surface was rescanned to observe any possible topography change. For the measurements presented below, no indication of atomic changes on the sample was observed.²⁵

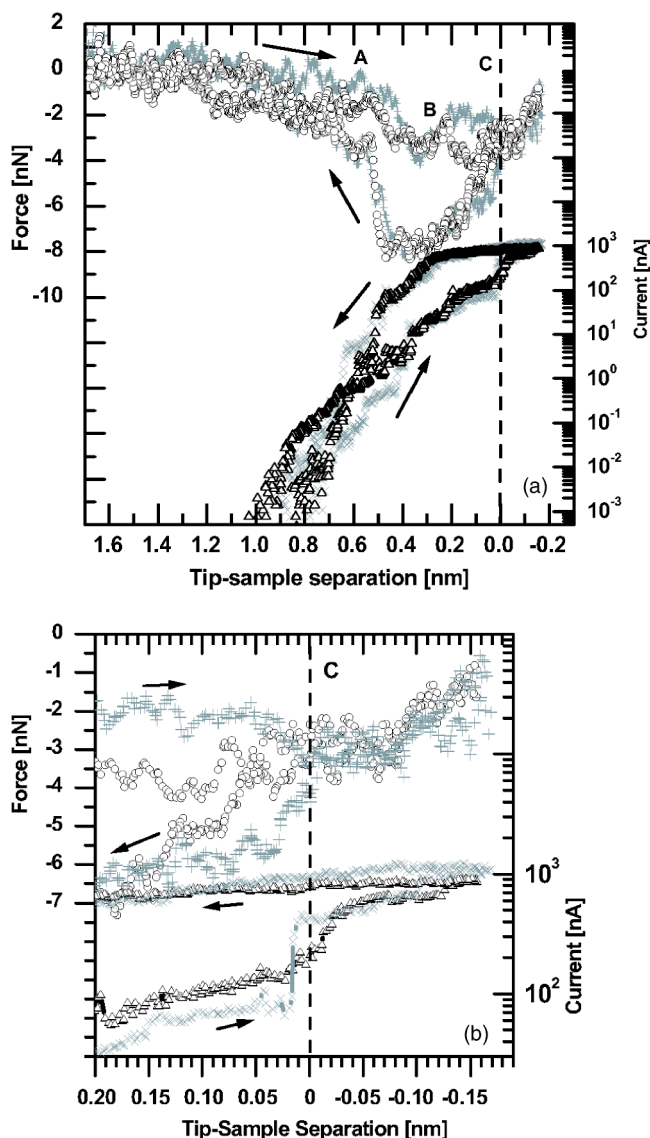


FIG. 1. Simultaneously acquired force-distance $F(z)$ and current-distance $I(z)$ curves covering a large tip-sample separation up to elastic contact (a), bias 50 mV; zoom the contact regime (b), where $F(z)$ curves are \circ and $+$, with corresponding $I(z)$ curves represented by \triangle and \times , respectively. The force signals are notched filtered at 60 and 180 Hz to remove the electronic noise.

Drift was below 2 nm/h in the X, Y, and Z directions.

In the following figures, the difference between cantilever deflection and STM piezo motion is plotted and referred to as the tip-sample separation. Note that this corresponds to the true change in tip-sample separation only if all atomic positions remain rigid and thus do not relax.

A representative selection of two consecutive approach-retraction cycles is shown in Fig. 1. At large distances, the interaction is dominated by van der Waals (vdW) forces. Calculations of vdW forces based on a sphere-plane model, a gap of 0.6 nm and an experimentally determined force of ~ 1 nN yield a tip radius of ~ 7 nm, consistent with estimates from field emission data for this tip. Capacitive (i.e., electrostatic) forces are excluded, as a sphere-plane model using a tip radius of 10 nm and a bias of 50 mV gives an

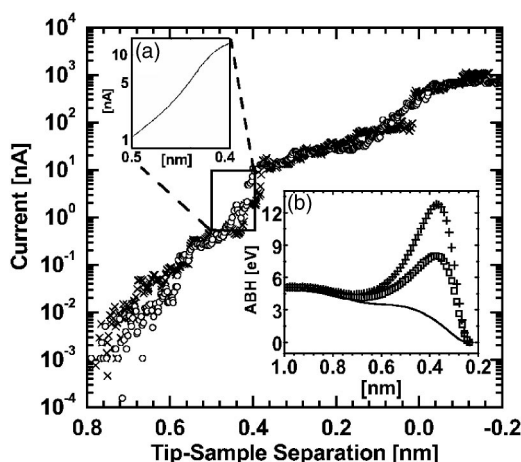


FIG. 2. Current-distance characteristics. Inset plots are theoretically calculated (a) current (from Ref. 13) and (b) work functions (ABH) vs tip-sample separation. Relaxation effects are more pronounced over top site (cross, b) than hollow site (square, b). The calculated work functions (without relaxation) do collapse (solid line, b).

electrostatic force < 0.01 nN, much less than the forces observed here. The tunneling current increased exponentially with an apparent barrier height (ABH) of 4.4 ± 0.8 eV.

Upon further approach from 0.6 to 0.3 nm strong metallic adhesion forces start playing a dominating role. For this particular tip, the current jumps from 0.1 nA to 10 nA in a staircase-like fashion. Approximately 0.1 nm prior to the jumps, the ABH is observed to decrease. After the jumps in current, the force rapidly increases and reaches a maximum attractive value of -3.5 ± 1.0 nN, indicating a sharp tip with an apex of approximately 1-3 atoms.¹⁵ During the staircase jumps (details in Fig. 2) the ABH is found to increase rapidly to 9.4 ± 2.0 eV. *Ab initio* simulations (details in Ref. 13) demonstrated that strong relaxation effects account for the rapid increase of ABH prior to the potential barrier collapse [Fig. 2(b)]. The calculated current [Fig. 2(a)] and ABH [Fig. 2(b)] as a function of tip-sample separation z match the experimental results quantitatively without any adjustable parameter (see below for the experimental determination of $z=0$ nm). The large increase in ABH is only due to a mechanical relaxation effect, the electronic barrier collapses as expected [solid line in Fig. 2(b)].

In the regions where strong metallic adhesion dominates (0.6–0.3 nm separation) the current approach and retraction paths are less well defined. On some cycles crossovers of paths are even observed. This is an indication that, in this intermediate region, significant charge redistribution and atomistic rearrangement of tip atoms can occur. The short-range attractive interaction [with decay lengths of typically 0.2 nm (see Refs. 15–17)] is due to exchange correlation forces, ultimately leading to the formation of metallic adhesion or chemical bonds. Note that this is typically the closest tip-sample separation in published NC-AFM interaction-distance curves.^{26,27} We observe no measurable approach-retraction hysteresis within the noise on either the $F(z)$ or the $I(z)$ channel if the tip is not approached beyond the point of maximum adhesion. This also indicates that piezo hysteresis or creep is negligible in these experiments.

During further approach, strong short-range repulsive forces set in at point B, changing the interaction force gradient to positive. The current increased steadily with an ABH of 0.4 ± 0.1 eV. This region is usually referred to as the potential barrier collapse regime characterized by significant electronic and mechanical interactions. Standard tunneling theories assuming unperturbed electrodes break down in this regime. It is, however, the regime relevant for molecular electronics. One would need modeling using, e.g., the Landauer formalism,²⁸ with calculation of the transmission coefficient taking the atomic structure of electrodes (tip and sample) into account.²⁹ Upon further approach of the tip to the sample, bonding states start to dominate antibonding states and thus lowering the total energy of the system, until a bond is formed between the tip and the sample. This manifests itself as a substantial increase in attractive force (partially offsetting the increased repulsive interactions) and a jump in current of about one order of magnitude, shown in detail in Fig. 1(b), point C.

The strong correlation between current and forces indicates, as expected, that the formation of an electrical contact is accompanied by the formation of a well-defined mechanical bond. Further compression of the contact yields minor changes in current. Mechanically, the contact is elastic in this regime: approach and retraction paths are indistinguishable. The slope of $F(z)$ in the elastic contact regime yields a contact stiffness of the order of 20 ± 6 N/m, giving an estimated interaction stiffness of the order of ~ 40 N/m. It should be pointed out that the front tip atoms and surface atoms contacted each other at point B, even earlier than point C, as confirmed by theoretical simulations.¹³ An experimental manifestation of this is the change in force gradient at B. However, a stable, reproducible, and well-defined mechanical and electrical contact point was only established when the second and third layers of tip and surface atoms recovered their equilibrium positions under the competition of attractive and repulsive interactions with various decay lengths. Note how the total relaxation of 0.3 nm between A and B is recovered between B and C. This value is close to the 0.2 nm relaxation predicted in Ref. 13.

We define point C as the point of contact and assign it a tip-sample separation of 0 nm [Fig. 1(b)]. The mechanical and electrical contact point differ by ~ 0.01 nm, equivalent to the uncertainty and thus to the error in the measurement. This zero tip-sample separation point is usually chosen arbitrarily.^{4,15,16} The observed conductance at the electrical contact point is 10% of the unit of quantum conductance G_0 [Fig. 1(b)], a value often observed in W break junctions.¹⁸ For atomically ill-defined tips, we experimentally observe variations in the maximum adhesion force as well as the magnitude of the contact force when the effective barrier breaks down and a well-defined contact is formed. Furthermore, the absolute conductance of such a contact can vary substantially, even for the same nominal force. Experimentally, the atomic structure of the tip needs to be characterized to allow quantitative comparison with modeling. Careful theoretical simulations, taking into account detailed atomic structure of both tip and sample surface electronic properties, charge transfer as well as relaxation effects are needed to fully explore this conductance regime.

The major difference between retraction and approach is the observation of a large hysteresis with a maximum attractive force of -8.0 ± 2.5 nN. Yet, after repeated approach curves, the point of contact is located at the same absolute separation to within the noise limit of 0.02 nm. Jumps both during approach as well as retraction in $I(z)$ and $F(z)$ are always on the subnanometer level, indicative of atomic level phenomena. We exclude the formation of a Au nanowire between tip and sample, as no change on the Au surface is detectable.²⁵ W is known to exhibit extreme mechanical robustness in nanojunctions due to its high yield strength, which however does not exclude elastic relaxation effects.^{13,18,30,31} The magnitude and distance characteristics of the retraction curves as well as the amount of hysteresis match previously published results obtained using a slightly sharper W(111) tip.^{15,16}

We speculate that the repulsive and/or strong adhesive forces acting on the tip apex of an atomically ill-defined tip during contact formation can lead to a bistable tip atomic configuration. After contact formation, a modified tip (in a bistable state) is potentially susceptible to large relaxation effects leading to substantial length increases, as are indeed observed, as a result of the short-range adhesive interaction. Simulations also showed that the relaxation effect is more pronounced in W(110) than W(111) due to its much more open structure.³¹ When the tip is far from the surface, the bistable state relaxes back into its lower-energy configuration, resulting in the initial tip structure, force and current return to their initial values. Similar tip instabilities may also account for the dissipation often observed in NC-AFM measurements.^{19,32}

In conclusion, we investigated in detail the interplay between current and interaction forces in the regimes from weak coupling to point contact between a W tip and a Au(111) sample. Based on the simultaneously recorded current and force responses, we can determine the electrical and mechanical contact points, which are found to coincide within measurement uncertainties. This allows us to compare with modeling without having to use any adjustable parameters as a well-defined zero separation point is established. In the tunneling regime, for separations larger than 0.4 nm, our experimental results are in quantitative agreement with modeling if relaxation effects are accounted for. The magnitude as well as the distance dependence of the observed force clearly has an important effect on the electron transport properties of this system. Molecules have much smaller elastic constants than metals, thus will easily be deformed by the measured nanonewton forces. When contacted with a tip, they are expected to show a large variability in electron transport properties depending on the magnitude and distance dependence of forces, which are a function of detailed tip geometry. If molecular structure-function relationships are to be extracted from comparison with modeling, nonuniform and nonlocal structural deformations due to the various forces and their associated, different decay lengths as well as their effects on molecular electronic states need to be taken into account. Our measurements provide a clear picture of the electronic transport and interactions between tip and sample at the atomic scale and should stimulate more experimental and theoretical efforts to address this fundamental issue.

The work is supported by the Natural Science and Engineering Research Council (NSERC) of Canada, the Canadian Institute of Advance Research (CIAR), Nano-Québec and the Regroupement Québécois sur les Matériaux

de Pointe (RQMP). We appreciate the excellent electronics designed and built at the Physics Department of the University of Basel under the expert guidance of H. Hidber.

-
- ¹*Scanning Tunneling Microscopy I, II, III*, edited by R. Wiesendanger and H. J. Güntherodt (Springer-Verlag, New York, 1993); H. Hug, R. Bennewitz, and E. Meyer, *Scanning Probe Microscopy: The Lab on a Tip* (Springer-Verlag, New York, 2003).
- ²J. K. Gimzewski and C. Joachim, *Science* **283**, 1683 (1999).
- ³A. Nitzan and M. A. Ratner, *Science* **300**, 1384 (2003).
- ⁴*Forces in Scanning Probe Methods*, edited by H. J. Güntherodt, D. Anselmetti, and E. Meyer, NATO Advanced Study Institute, Series E: Applied Science (Kluwer Academic Publishers, Dordrecht, 1994), Vol. 184.
- ⁵C. J. Chen, *Introduction to Scanning Tunneling Microscopy* (Oxford University Press, New York, 1993).
- ⁶U. Dürig, *IBM J. Res. Dev.* **38**, 347 (1994); U. Dürig, O. Züger, and D. W. Pohl, *Phys. Rev. Lett.* **65**, 349 (1990).
- ⁷G. Binnig, N. Garcia, H. Rohrer, J. M. Soler, and F. Flores, *Phys. Rev. B* **30**, 4816 (1984).
- ⁸G. Rubio, N. Agraït, and S. Vieira, *Phys. Rev. Lett.* **76**, 2302 (1996).
- ⁹L. Olesen, M. Brandbyge, M. R. Sørensen, K. W. Jacobsen, E. Lægsgaard, I. Stensgaard, and F. Besenbacher, *Phys. Rev. Lett.* **76**, 1485 (1996).
- ¹⁰J. K. Gimzewski and R. Möller, *Phys. Rev. B* **36**, R1284 (1987); N. D. Lang, *Phys. Rev. B* **36**, R8173 (1987).
- ¹¹S. Ciraci, *Ultramicroscopy* **42–44**, 16 (1992); **42–44**, 163 (1992); S. Ciraci and E. Tekman, *Phys. Rev. B* **40**, R11 969 (1989); A. Buldum, S. Ciraci, C. Y. Fong, and J. S. Nelson, *Phys. Rev. B* **59**, 5120 (1999).
- ¹²W. A. Hofer, A. S. Foster, and A. L. Shluger, *Rev. Mod. Phys.* **75**, 1287 (2003).
- ¹³W. A. Hofer, A. J. Fisher, R. A. Wolkow, and P. Grütter, *Phys. Rev. Lett.* **87**, 236104 (2001); W. A. Hofer and A. J. Fisher, *Phys. Rev. Lett.* **91**, 036803 (2003).
- ¹⁴U. Landman, W. D. Luedtke, N. A. Burnham, and R. J. Colton, *Science* **248**, 454 (1990).
- ¹⁵A. Schirmeisen, G. Cross, A. Stalder, P. Grütter, and U. Dürig, *New J. Phys.* **2**, 29 (2000).
- ¹⁶G. Cross, A. Schirmeisen, A. Stalder, P. Grütter, M. Tschudy, and U. Dürig, *Phys. Rev. Lett.* **80**, 4685 (1998).
- ¹⁷B. Gotsmann and H. Fuchs, *Phys. Rev. Lett.* **86**, 2597 (2001).
- ¹⁸A. Halbritter, Sz. Csonka, G. Mihaly, E. Jurdik, O. Yu. Kolesynchenko, O. I. Shklyarevskii, S. Speller, and H. van Kempen, *Phys. Rev. B* **68**, 035417 (2003).
- ¹⁹*Noncontact Atomic Force Microscopy*, edited by S. Morita, R. Wiesendanger, and E. Meyer (Springer-Verlag, New York, 2002).
- ²⁰A. Stalder, PhD thesis, University of Freiburg, Switzerland, 1995.
- ²¹U. Dürig, L. Novotny, B. Michel, and A. Stalder, *Rev. Sci. Instrum.* **68**, 3814 (1997).
- ²²A. S. Lucier, MSc thesis, McGill University, Canada, 2004; A. Schirmeisen, PhD thesis, McGill University, Canada, 1999.
- ²³J. M. Mativetsky, S. A. Burke, R. Hoffmann, Y. Sun, and P. Grütter, *Nanotechnology* **15**, S40 (2004).
- ²⁴A customized version of the all-digital *Scanita* electronics was designed and built at the University of Basel.
- ²⁵A few gold atoms missing will change the reconstruction pattern, which can be easily observed by STM. Y. Hasegawa and Ph. Avouris, *Science* **258**, 1763 (1992).
- ²⁶S. P. Jarvis, H. Yamada, S. I. Yamamoto, H. Tokumoto, and J. B. Pethica, *Nature (London)* **384**, 247 (1996).
- ²⁷M. A. Lantz, H. J. Hug, R. Hoffmann, P. J. A. van Schendel, P. Kappenberger, S. Martin, A. Baratoff, and H.-J. Güntherodt, *Science* **291**, 2580 (2001).
- ²⁸S. Datta, *Electron Transport in Mesoscopic Systems* (Cambridge University Press, New York, 1995).
- ²⁹J. Taylor, H. Guo, and J. Wang, *Phys. Rev. B* **63**, 245407 (2001).
- ³⁰The maximum negative force gradient is -15 N/m, much smaller than the cantilever spring constant of 45 N/m.
- ³¹Field-ion microscopy studies show that tip apexes of electrochemically etched and annealed polycrystalline W tips are always (110) oriented. See Ref. 22 for more details.
- ³²N. Sasaki and M. Tsukada, *Jpn. J. Appl. Phys., Part 2* **39**, L1334 (2000); see also Chap. 19 in Ref. 19.